Performance Characteristics of Electrochemically Prepared Tin Fluoborate

By S.M. Silaimani, M. Pushpavanam and K.C. Narasimham

Among the metals widely used in plating, tin is one of the most important because it plays a key role in the electronics and can-manufacturing industries, and because of its good solderability and excellent corrosion resistance in a variety of atmospheres. The authors suggest that an electrochemically prepared tin plating solution is superior to a commercial product.

Electroplating of tin from a fluoboric acid bath is preferred, mainly because of the solubility of the salt, which increases the operating current density and the rate of deposition, as experienced in high-speed plating. The bath is quite stable and no sludge forms on the anode. Generally, tin fluoborate required for the bath is prepared by chemical method,[1-5] which gives rise to numerous problems[6,7] during bath preparation and electroplating, resulting from the presence of contaminants. A suitable electrochemical method of preparing tin fluoborate has been standardized by the authors.[8]

In this paper, the performance characteristics of tin fluoborate electrolyte prepared by an electrochemical method are compared with those of commercial tin fluoborate solutions, with reference to (1) the solution properties (*i.e.*, effect of impurities, free acid concentration, etc.) and (2) deposit properties (*i.e.*, porosity, corrosion resistance, solderability, reflowing ability). The surface morphology of the deposits was studied by SEM and XRD methods.

Experimental Procedure

Hull Cell experiments were conducted to optimize the current density at which desired deposits could be obtained, using electrochemically prepared tin fluoborate (Bath A) as well as commercial tin fluoborate (Bath B). A 267-mL Hull Cell was used at a plating current of 2 A and duration 5 min., using an electrolyte of the following composition:

Tin fluoborate: 80 g/L (as tin)
Free fluoboric acid: 125 g/L
Gelatin: 6 g/L
Beta-naphthol: 1 g/L

Deposition was carried out by varying the free acid concentration and metal content. The effects of metallic impurities, such as Zn^{+2}, Fe^{+2} and Ni^{+2}, were also evaluated.

Throwing Power

The throwing power of the electrolytes was compared, using the Haring-Blum Cell at a current density of 1 A/dm^2. The percentage of throwing power was calculated using Fields' formula. Experiments were conducted at various free acid concentrations.

Electroplating of Tin

Deposition was carried out from Baths A and B at various current densities, (1, 2 and 3 A/dm^2) and at various free acid concentrations, (125, 150 and 175 g/L), by passing a fixed quantity of electricity with the help of a coulometer and a regulated power supply. Experiments were carried out only at room temperature. From the gain in weight, the efficiency was calculated.

Properties of Electroplated Tin

Porosity

Porosity of the electroplated tin, coated over steel, from the two baths, was detected by the following tests:

1. Ferroxyl test
2. Hot water test
3. Electrographic test

Special test papers were prepared[9] by impregnation in a solution containing 50 g/L NaCl and 50 g/L gelatin and drying. They were rewetted in 50 g/L NaCl solution again just before the test, then pressed against the electrodeposited panel and left for 10 min. The papers were immersed in 10 g/L solution of potassium ferricyanide. Blue marks developed in the region where steel was exposed through discontinuities in the coating, were counted by examining the surface in a microscope at 10X magnification. The porosity of the coating was expressed as the percentage defective area.

The coated specimens were immersed in hot water at 95 °C for six hr; the pores in the deposit were examined by metallurgical microscope.

The special paper prepared above was sandwiched between the anode (*i.e.*, the test specimen) and an aluminum foil cathode. A current density of 5 mA/dm^2 was applied for 3 min. The paper was then developed with potassium ferricyanide. The percentage defective area was calculated as described earlier. Panels with coating thicknesses of 2.5, 3.5 and 5 µm were used for testing porosity.

Solderability

Panels with coating thickness of 2.5, 3.5, 5 and 10 µm obtained from the two baths were used for testing solderability, which was measured by placing a fixed volume of solder on the test specimen, which was heated to 240 °C. The solder melted and spread over the surface. The sample was then cooled, and the area of spread was measured with a planimeter. Spread factor for a particular test surface was calculated by using the equation:

$$\text{Percent spread factor} = \frac{D - H}{D} \times 100$$

where D is the diameter of the sphere having a volume equal to that of the solder used and H is the height of the solder sphere. The solderability of the coatings was rated as suggested in the literature.[10]

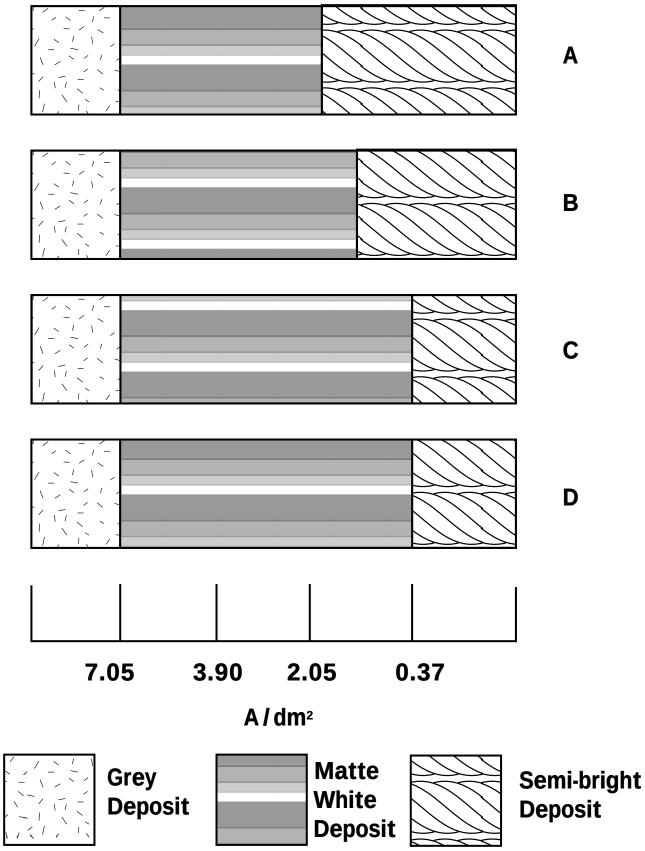

Fig. 1—Hull Cell pattern from electrochemically prepared tin fluoborate solution (Bath A) at various free acid concentrations: (a) 100 g/L; (b) 125 g/L; (c) 150 g/L; (d) 175 g/L.

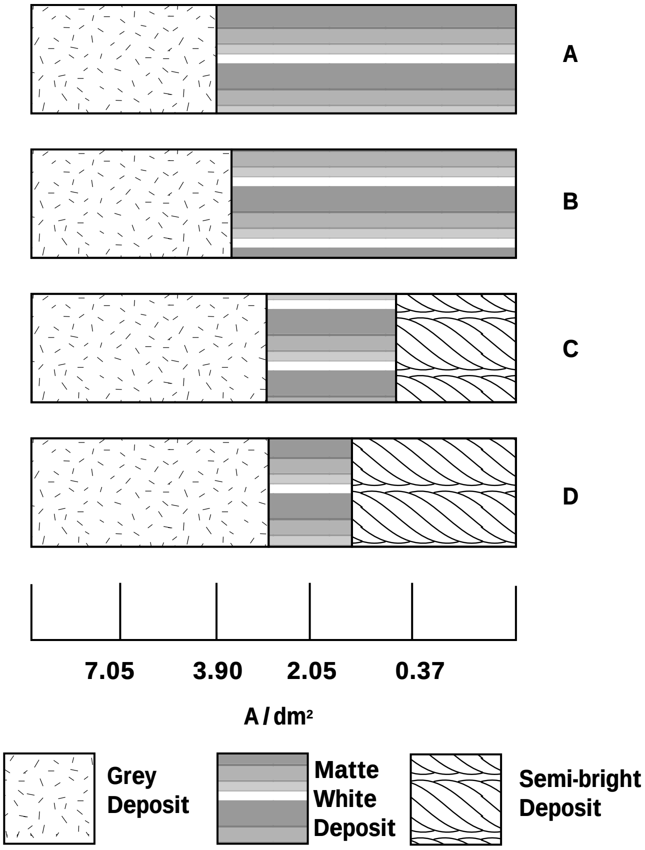

Fig. 2—Hull Cell pattern from commercial tin fluoborate solution (Bath B) at various free acid concentrations: (a) 100 g/L; (b) 125 g/L; (c) 150 g/L; (d) 175 g/L.

Reflowing

Panels with coating thicknesses of 1.0, 1.75 and 2.5µm were flow-melted in a palm oil bath maintained at a temperature of 240-260 °C for 10 sec, then water-quenched. This treatment helped in filling even the small pores in the deposit and produced a lustrous finish. A bright, smooth coating completely covering the surface indicates acceptable quality.[11] The coating reflectivity is measured after flow-melting using a UV-visible-NIR spectrophotometer. The light source used was a tungsten-iodine lamp. A high-alumina pellet was used as the reference mode.

Corrosion Resistance Studies

The corrosion resistance of coatings 2.5, 3.5, 5.0 and 10.0 µm in thickness were estimated by potentiodynamic method, using a bioanalytical system. The potentials were scanned over 150 mV, in both the cathodic and anodic directions from the open-circuit potentials with suitable IR corrections. The intercepts of the linear portions of the two polarization curves give i_{corr} and E_{corr} values.[12]

The corrosion resistance of deposits with thicknesses of 5 and 10 µm were also assessed by conducting salt spray experiments in 5-percent sodium chloride solution, with 8 hr spraying followed by 16 hr rest. The hours of spraying, as well as total hours spent in the cabinet until the onset of failure of the sample, as indicated by red rust formation, were recorded. The corrosion resistance of the panels was evaluated according to ASTM standards.[13]

The surface morphology of the electrodeposits obtained from the two baths was examined under higher magnification to assess the grain size, nature of deposit, and number of pores, using a scanning electron microscope. X-ray diffraction (XRD) with CuKα radiation was used to understand the phase orientation and lattice parameters of the deposits.

Results and Discussion

The Hull Cell pattern obtained in the absence of any addition agent showed high whisker growth, with a non-coherent deposit. In the presence of β-naphthol (1 g/L) and gelatin (6 g/L), the whisker growth totally disappeared, yielding matte white and semibright deposits in the high- and low-current density regions, respectively. The Hull Cell patterns obtained from electrochemically prepared tin fluoborate (Bath A) is shown in Fig. 1 (a, b, c and d). It is evident from this figure that as the free acid concentration increases from 100 to 150 g/L, the current density region for the semibright deposit decreases, yielding a wider current density range for getting a matte white deposit. This trend is observed only up to 150 g/L free fluoboric acid; further increase in concentration yields only an insignificant difference. These results suggest that a free acid concentration of 125 to 150 g/L is optimum for a satisfactory deposit.

The Hull Cell patterns obtained from the commercial tin fluoborate bath in the presence of same addition agents show a slight difference (Figs. 2a-d). As the free acid concentration is increased from 100 to 150 g/L, the matte white deposit is present over the entire range. Only above 150 g/L of free acid are semibright deposits obtained in the low-current-density region. This difference is explained on the basis of impurities present in the electrolyte.

It must be mentioned here that the commercial bath containing 100 g/L of free acid becomes slightly turbid after the experiment. This may be because of insufficient free acid to solubilize the stannous ion at the cathode, resulting in precipitation of tin hydroxide, the cause of the turbidity. Consequently, the deposit obtained from the bath containing 100 g/L free acid is rough, a likely result of incorporation of the precipitate.

In an electrochemically prepared fluoborate bath, when the metal concentration in the solution is increased from 50 to 100 g/L, while maintaining the free acid content at 125 g/L, current densities for both semibright and matte white deposits shift to a higher value, from 5 A/dm^2 to above 8 A/dm^2, resulting in reduction of the grey powder formation (Figs. 3a-c).

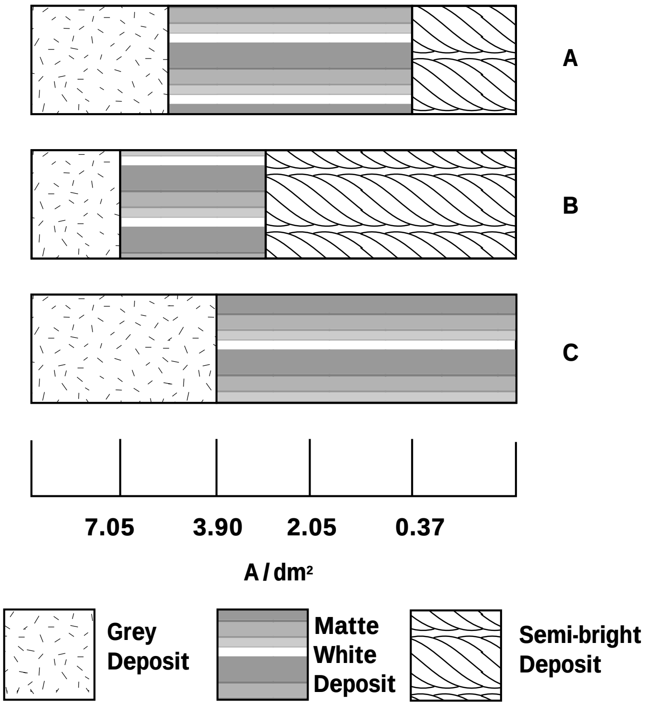

Fig. 3—Hull Cell pattern from Bath A at various tin concentrations: (a) 40 g/L; (b) 80 g/L; (c) 120 g/L.

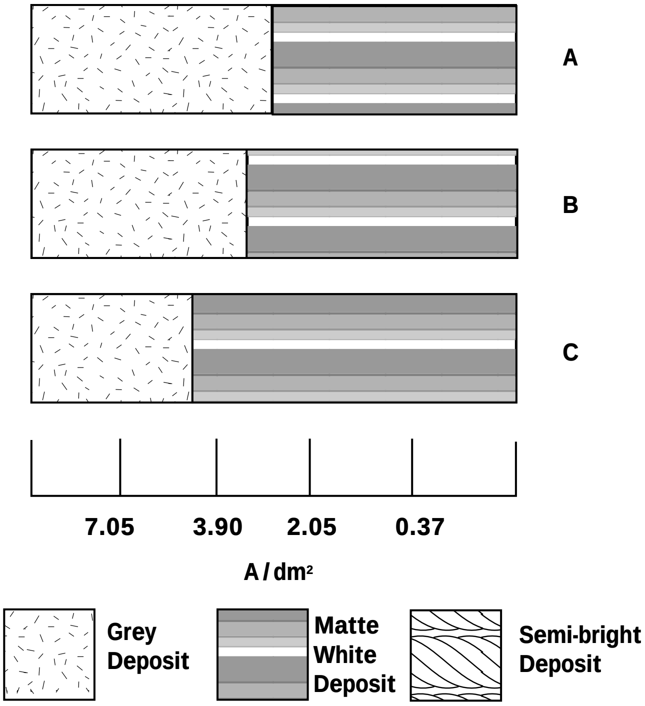

Fig. 4—Hull Cell pattern from Bath B at various tin concentrations: (a) 40 g/L; (b) 80 g/L; (c) 120 g/L.

In the commercial tin fluoborate bath, a complete matte white deposit only is obtained with increase in tin content (Figs. 4 a-c).

Throwing Power

The results of the throwing power experiments given in Table 1 indicate that the tin fluoborate solution prepared by electrochemical method (Bath A) offers better throwing power than the commercial tin fluoborate solution. Table 2 shows that the current efficiency of the deposit decreases with increase of free acid concentration. The two baths under

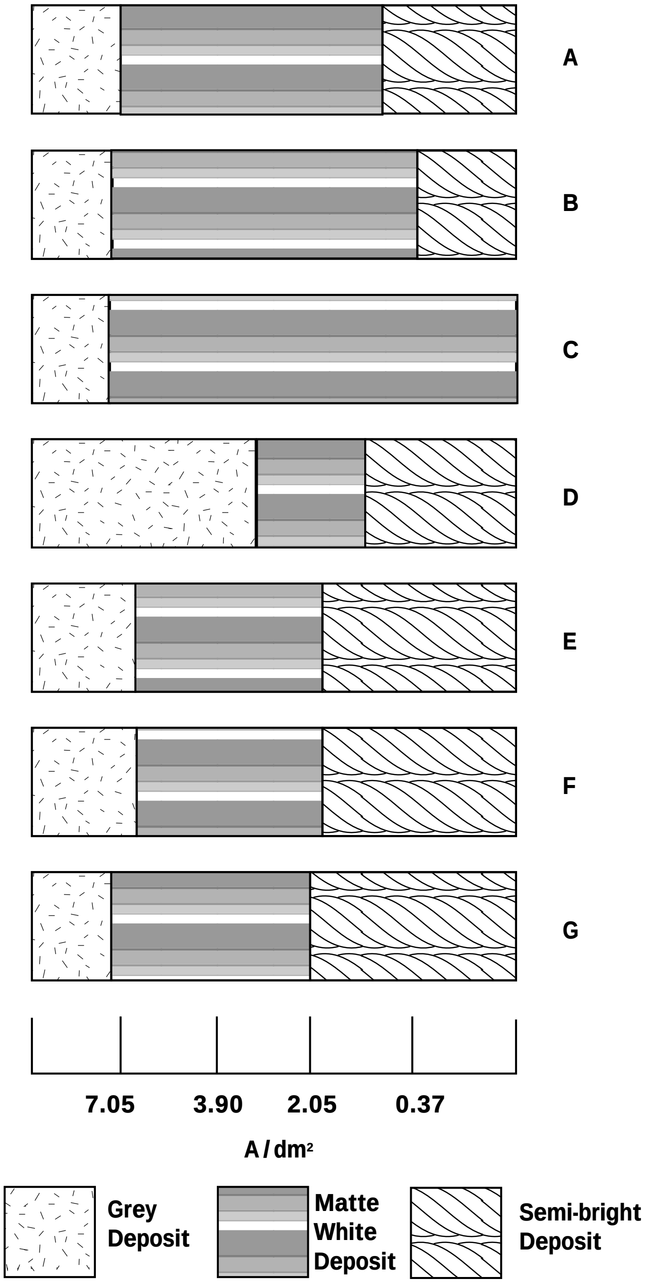

Fig. 5—Effect of various metallic impurities: (a) 0.4% Zn^{+2}; (b) 0.8% Zn^{+2}; (c) 1.2% Zn^{+2}; (d) 0.04% Ni^{+2}; (e) 0.04% Fe^{+2}; (f) 0.08% Fe^{+2}; (g) 0.12% Fe^{+2}.

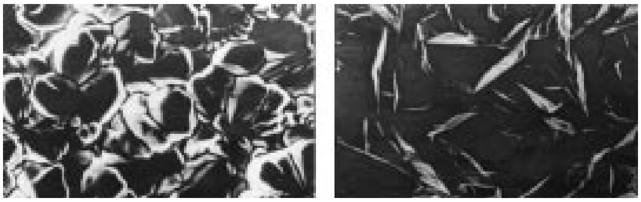

Fig. 6—SEM photomicrographs of tin deposits: (a) from bath A; (b) from Bath B

study show the same trend that results from increased hydrogen evolution. The lower efficiency of Bath B, compared to Bath A, however, can be a result of the presence of impurities.

Effect of Impurities

Analysis of the two electrolytes shows that zinc, nickel and iron are present as trace impurities above the specified level in electrolyte B.[7] These impurities may have modified the Hull Cell pattern of the Bath B. This is further confirmed by the addition of known quantities of the metal impurities to bath A; the Hull Cell patterns obtained are shown in Fig. 5.

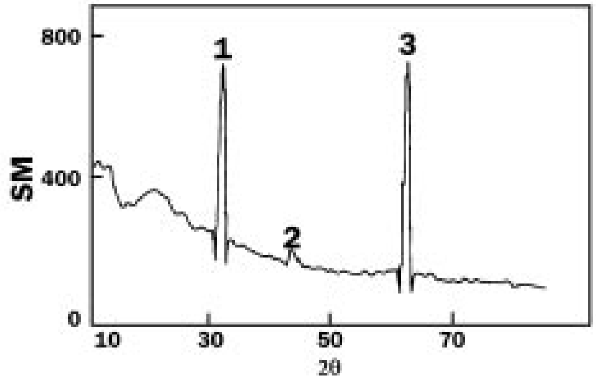

Fig. 7—X-ray diffraction pattern of deposit from Bath A.

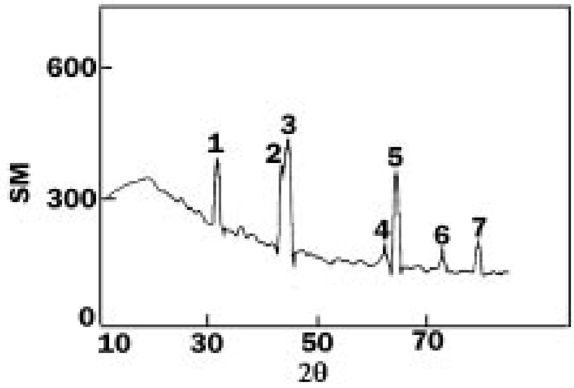

Fig. 8—X-ray diffraction pattern of deposit from Bath B.

Addition of zinc to Bath A modifies the semibright nature of the deposit in the lower current density region to a matte white, with increase of Zn^{+2} concentration (Figs. 5a-c). Addition of nickel results in extending the gray powdery pattern toward less-current-density regions (Fig. 5d). There is no marked difference in the pattern with addition of Fe^{+2} at concentrations between 0.04 and 0.12 percent (Figs. 5e-g).

Porosity

The results of all three tests listed in Table 3 indicate that the porosity of the deposits decreases as the thickness is increased from 2.5 to 5 µm. The results of the hot water test are slightly on the higher side compared to the other tests, which may be a result of the higher temperature and extended duration of the test. The deposit obtained from Bath B is more porous than that from Bath A. This can be attributed to the presence of impurities in Bath B and this was further confirmed by structural examination.

Table 1
Throwing power of Tin Fluoborate Baths

Solution	Concentration free HBF4, g/L	% throwing power 1 A/dm^2
Bath A		
1.	125	45.2
2.	150	50.7
3.	175	56.3
Bath B		
1.	125	37.7
2.	150	45.4
3.	175	51.1

Table 2
Cathode Current Efficiency

Solution	Concentration free HBF_4, g/L	% Current Efficiency 1 A/dm^2	2 A/dm^2	3 A/dm^2
Bath A				
1.	125	99.4	98.9	97.6
2.	150	96.7	96.5	96.0
3.	175	95.9	95.6	95.6
Bath B				
1.	125	97.2	95.6	94.1
2.	150	94.6	93.6	91.6
3.	175	89.9	87.4	86.5

Table 3
Porosity at Different Coating Thicknesses

Solution	Coating thickness, µm	% Defective area Chemical method	Electrographic method	Hot water
Deposit from Bath A				
1.	2.5	10	14	16
2.	3.5	8	8	10
3.	5.0	2	3	5
Deposit from bath B				
1.	2.5	24	29	33
2.	3.5	14	20	25
3.	5.0	6	9	13

Table 4
Polarization Behavior of Tin Coating

Solution	Coating thickness, µm	E_{corr} mV	I_{corr} mA
Bath A			
1.	2.5	-575	4.59×10^{-3}
2.	3.5	-545	1.59×10^{-3}
3.	5.0	-539	7.33×10^{-3}
Bath B			
1.	2.5	-582	1.46×10^{-2}
2.	3.5	-566	9.07×10^{-2}
3.	5.0	-558	1.23×10^{-2}

Table 5
Salt Spray Results

Solution	Deposit Thickness µm	Protective rating No.	Appearance rating No.
1. Bath A	5	5.6	4.4
2. Bath A	10	7.1	6.1
3. Bath B	5	4.5	4.0
4. Bath B	10	6.7	5.6

Table 6
Solderability

Soln.	Coating thickness µm	Dia. solder sphere mm	Sphere height (H) mm	% Spread factor	Remarks
Bath A					
1.	2.5	7.98	2.4	69.9	Fair
2.	3.5	8.74	1.8	79.4	Good
3.	5.0	10.09	1.0	90.1	Excellent
4.	10.0	10.09	1.0	90.1	Excellent
Bath B					
1.	2.5	6.18	3.4	45.0	Very poor
2.	3.5	7.14	2.8	60.8	Fair
3.	5.0	7.78	1.6	70.9	Good
4.	10.0	7.78	1.6	70.9	Good

$$\% S = \frac{D - H}{D} \times 100$$

Table 7
Reflectivity after Flow Melting

Solution	Coating thickness	% Transmittance, µm
Bath A		
1.	1.00	30.2
2.	1.75	28.4
3.	2.50	6.9
Bath B		
1.	1.00	20.0
2.	1.75	18.7
3.	2.50	7.9

Table 8
X-ray Diffraction Results

Solution	2θ	d	hkl	Lattice parameters
A. Electrochemically prepared bath				
1.	31.500	2.838	101	6.200
2.	43.800	2.063	220	5.834
3.	62.100	1.493	112	6.110
B. Commercial bath				
1.	31.600	2.829	101	6.097
2.	43.800	2.063	220	5.834
3.	44.300	2.034	(This peak corresponds to iron)	
4.	61.980	1.498	112	6.290
5.	64.200	1.450	400	6.980
6.	72.600	1.301	420	5.810
7.	79.200	1.208	312	5.870

$$a = \frac{h^2 + K^2}{1/2h + l^2/C^2}$$

Corrosion Tests

Potentiodynamic Polarization

The results of potentiodynamic polarization are summarized in Table 4. As the coating thickness is increased from 2.5 to 10 µm, the corrosion current decreases by as much as 5 µm; thereafter it remains constant in both cases. These numbers support the porosity results. The corrosion current for the deposits from Bath B is always higher.

Salt Spray

The results of the salt spray test conducted for 1680 hr are shown in Table 5. The appearance rating of the deposit obtained from Bath B at a thickness of 5 µm is "4," while the deposit obtained from bath A is 4.4. For a thickness of 10 µm, the recommended ASTM rating to pass the test is "4." The deposit obtained from Bath A meets this requirement, even at a thickness of 5 µm. A similar result is obtained with thickness of 10 µm also, indicating that the deposits obtained from Bath A are superior to those from Bath B. Even though the appearance rating in both cases is around "4," for a thickness of 5 µm, the protective rating is poor for the deposit from bath B. These results confirm the results obtained by porosity tests.

Solderability

Table 6 lists the solderability of tin deposits of various thicknesses obtained from the two baths, A & B. Note that the percentage spread factor increases from 69.9 to 90 percent in the case of deposits obtained from Bath A and from 45 to 70.9 percent in the case of deposits obtained from Bath B, with increase of thickness from 2.5 to 5 µm. These results imply that a tin coating with better solderability is obtained from Bath A. The results of solderability of the coating agree well with the porosity results as expected, because solderability depends on thickness and porosity.

Reflowing

After flow melting, the reflectivity of the deposit drastically decreases after 1.75 µm, which is the result of formation of distinct beads in the case of deposit from Bath A and matte patches with slight beads from bath B (Table 7). For deposits from Bath A, the thickness can be well below 2.5 µm to obtain smooth, glossy pore-free flow melting, whereas the deposit from Bath B needs greater thickness.

Morphology

SEM photomicrographs of the deposit obtained from Baths A & B with thickness of 10 µm are shown in Fig. 6. The deposit obtained from Bath A has more uniformly spaced grain size with no voids, whereas the deposit from Bath B shows needle-like structure with many voids. The difference in structural morphology can be attributed to the difference in behavior with respect to porosity, solderability, flow melting and corrosion resistance of the coating.

X-ray Diffraction Patterns

The X-ray diffraction patterns of the deposits obtained from Baths A & B (Figs. 7 & 8) show noticeable differences. The two-theta values are shifted and numerous peaks are observed in the deposits from Bath B. Although the presence of impurities in the deposit is not distinct, it can be concluded from the presence of numerous peaks that the direction of crystal orientation is different for the two deposits. The assorted orientations of the crystal may be the reason for the dullness of the deposit obtained from Bath B. The *hkl* values and average lattice parameters are shown in Table 8.

Findings

1. The Hull Cell patterns of the deposit from the electrochemically prepared bath differ from the commercial, as a result of impurities in the commercial bath. Under identical conditions, the current efficiency for the deposition and throwing power of the electrolyte prepared by electrochemical method is better than that obtained with the commercial electrolyte.
2. The deposits obtained from the electrochemically prepared tin fluoborate are less porous, more easily solderable and more corrosion resistant than those from the commercial bath.
3. The SEM photomicrographs show that the deposits from the electrochemically prepared fluoborate bath are more compact than those obtained from the commercial bath.

Editor's note: *Manuscript received, March 1996.*

References

1. J.W. Mellor, *A Comprehensive Treatise on Inorganic and Theoretical Chemistry*, Longmans Green & Co., New York, NY, 1964; Vol. 6, p. 128.
2. A.L. Ferguson, U.S. patent 2,457,798 (1949), *CA* **43**, 2745 (1949).
3. Andre Riesser, French patent 1,199,639 (1959), *CA* **55**, 9810 (1961).
4. Ullmanns, *Encyclopedia of Industrial Chemistry,* 5th Ed. p. 313-14, Elevers S. Hawkins and G. Schulz, New York (1991).
5. Kirk-Othmer, *Encyclopedia of Chemical Technology*, 3rd Ed., **23**, Wiley Interscience, New York, NY, 1983; p.490.
6. F.A. Lowenheim, *Modern Electroplating,* 3rd Ed., John Wiley & Sons, Inc., New York, NY, 1966.
7. J.P. Langres, *Plat. and Surf. Fin.,* **70**, 21 (Jan. 1983).
8. S.M. Silaimani, M. Pushpavanam and K.C. Narasimham, unpublished data.
9. V.E. Carter, *Metallic Coatings for Corrosion Control,* Newness, Butterworths, London, 1977.
10. R. Sard, O. Oglinn and S. Leidheiser, *Symp. Electrochem. Soc.*, (1974).
11. ASTM Standards 02-05 B537 (1985).
12. M. Stern and A.C. Geary, *J. Electrochem. Soc.,* **104**, 56 (1957).
13. ASTM Standards, 02-05 B545 (1985).

SUR/FIN® '97 Abstracts
Due November 1, 1996

Please send 75–100 word abstracts to:

Dr. I-yuan Wei or R.G. Baker, CEF-SE
AESF
12644 Research Parkway
Orlando, FL 32826-3298
e-mail: <72420.2001@compuserv.com

Silaimani

Pushpavanam

Narasimham

About the Authors

Dr. S.M. Silaimani is a research fellow/associate in the Industrial Metal Finishing Division of the Central Electrochemical Research Institute (CECRI), Karaikudi 630 006, Tamilnadu, India. She has published 10 papers in the area of metal finishing.

Dr. Malathy Pushpavanam is a researcher at the Central Electrochemical Research Institute. She has published more than 170 papers and holds 15 patents in metal finishing.

Dr. K.C. Narasimham is working as scientist emeritus at CECRI, having retired as deputy director and head of the Electrochemicals Division. He has published more than 150 research papers. He also holds 26 patents and has won five awards for developed processes.